*The object of this study is the process of electron beam 3D printing of articles made of TA15 titanium alloy powder. Peculiarities of the structure and properties formation of alloy blanks, obtained by this method have been described. Influence of process parameters (electron beam power and geometric scanning parameters) on the characteristics of the material were considered.*

*Step of displacement of the beam trajectory changed from 0.1 to 0.25 mm with an interval of 0.05 mm. Specific energy of the electron beam varied from 20 to 70 J/mm$^3$ for every trajectory displacement step.*

*The macrostructure was examined visually while the microstructure was studied by optical microscopy. Mechanical properties were determined by uniaxial tension and impact bending tests. It was established that depending on the 3D printing parameters the macrostructure of most samples is dense but with unfavorable parameters non-fusions or shrinkage porosity defects may form. The microstructure of the dendritic type has an α′+β lamellar-acicular morphology, its dispersity and shape of α′–phase areas vary depending on the process parameters.*

*A scanning step of 0.2 mm and a beam energy of 40 J/mm$^3$ allows obtaining a dispersed microstructure in which there are no non-fusions and shrinkage micropores. The value of the $R_m$ is 27 %, and the $R_{0.2}$ is 24 % higher than that of the alloy obtained by the conventional technology of electron beam melting. The $A_5$ is 3.2 times higher. However, impact toughness of the sample with dendrite unfavorable orientation to the direction of load applying may be lower compared to conventional technology. The results could be used for devising commercial technology of high strength titanium alloys parts produced by 3D printing*

*Keywords: electron beam 3D printing, titanium alloy, TA15, technological parameters, metallographic studies*

UDC 621.791.92
DOI: 10.15587/1729-4061.2024.306613

# DETERMINING TECHNOLOGICAL PARAMETERS FOR OBTAINING TA15 TITANIUM ALLOY BLANKS WITH IMPROVED MECHANICAL CHARACTERISTICS USING THE ELECTRON-BEAM 3D PRINTING METHOD

**Serhii Akhonin**
Academician of NAS of Ukraine, Doctor of Technical Sciences, Professor,
Deputy Director for Scientific Work
Department of Metallurgy and Welding of Titanium Alloys**
**Vladimir Nesterenkov**
Corresponding Member of the National Academy of Sciences of Ukraine,
Doctor of Technical Sciences, Senior Researcher, Head of Department*
**Volodymyr Pashynskyi**
*Corresponding author*
Doctor of Technical Sciences, Associate Professor, Head of Department
Department of Metallurgy, Material Science and Organization of Production
Technical University "Metinvest Polytechnic" LLC
Pivdenne highway, 80, Zaporizhzhia, Ukraine, 69008
E-mail: v.v.pashinskiy@mipolytech.education
**Vladyslav Matviichuk**
Researcher*
**Sviatoslav Motrunich**
PhD, Leading Engineer
Scientific-Technical Complex**
**Volodymyr Berezos**
Doctor of Technical Sciences, Leading Researcher
State Enterprise "Scientific-Production Center "Titan"
of the E. O. Paton Electric Welding Institute
of the National Academy of Sciences of Ukraine "
Raketna str., 26, Kyiv, Ukraine, 03028
**Illia Klochkov**
PhD
Department of Strength of Welded Structures**
*Department of Physical Processes, Technology
and Equipment for Electron Beam and Laser Welding**
**E. O. Paton Electric Welding Institute
of the National Academy of Sciences of Ukraine
Kazymyra Malevycha str., 11, Kyiv, Ukraine, 03150

*Received date 03.04.2024*
*Accepted date 14.06.2024*
*Published date 21.06.2024*

***How to Cite:*** *Akhonin, S., Nesterenkov, V., Pashynskyi, V., Matviichuk, V., Motrunich, S., Berezos, V., Klochkov, I. (2024). Determining technological parameters for obtaining TA15 titanium alloy blanks with improved mechanical characteristics using the electron-beam 3D printing method. Eastern-European Journal of Enterprise Technologies, 3 (12 (129)), 36–45. https://doi.org/10.15587/1729-4061.2024.306613*

## 1. Introduction

The use of 3D printing technologies is a promising direction for obtaining workpieces of complex shape, as close as possible to the dimensions of the final article. This technology can be used to produce parts based on a digital model obtained in automated design (CAD) systems directly at a 3D printing installation. This makes it possible to shorten

the technological process of obtaining the final article by eliminating some molding operations, such as casting or plastic deformation of the workpiece. It is also possible to reduce the amount of mechanical processing of the workpiece. But this imposes higher requirements on the quality of the macro- and microstructure of the material. To realize the advantages of 3D printing technology, it is necessary to enable the formation of a given structure already in the production process. Since the shape and dimensions of the final article are already formed, there is no possibility of adjusting the structure of the article by further plastic deformation.

When manufacturing articles from chemically active metals and alloys, it is necessary to use such technological processes that exclude the interaction of the material with the environment, which prevents the development of oxidation processes. From this point of view, the technology of layer-by-layer fusion of metals in a vacuum with an electron beam is very promising. It also makes it possible to control the process of product formation by changing many technological parameters, such as the type and parameters of the starting material for printing, the parameters of the material supply to the fusing zone, and the geometric and energy parameters of the electron beam. But such a multifactorial process requires determining the rational values of its parameters, which necessitates research into the regularities of the formation of a set of article characteristics. Therefore, research in this area is relevant for determining specific parameters of the process and, in the future, devising industrial technologies of electron-beam 3D printing. It is also necessary for advancing theoretical ideas about the mechanism of formation of the structure and properties of titanium alloy blanks when using this technology.

## 2. Literature review and problem statement

Determining the parameters of the technological process of layer-by-layer fusion of metals in a vacuum with an electron beam (electron beam melting) – a relatively new technology – is of great interest to researchers. In particular, in [1], the results of a comparative study of samples obtained by selective laser and electron beam melting, made from pre-alloyed, sprayed precursor powders, are reported. These include Cu, Ti-6Al-4V, alloy 625 (Ni-based superalloy), Co-based superalloy, and 17-4 PH stainless steel. These systems were studied by the methods of optical metallography, scanning and transmission electron microscopy, and X-ray diffraction. However, the study did not consider the issue of the formation of a set of physical and mechanical characteristics depending on the parameters of the melting process.

Another approach to the analysis of product formation processes using electron beam melting technology was devised in [2]. Material formation is analyzed from the point of view of heat and mass transfer processes. The authors built mathematical models of the formation of the molten bath and its crystallization, which allows predicting the state of the surface of articles. However, studies have been conducted for a variant of the technology when the surfacing material is introduced in the form of a wire. This does not make it possible to directly transfer the drawn conclusions to the surfacing process using powders.

In [3], the technological parameters that affect the quality of articles obtained by electron beam melting methods are considered; the classification of macro- and microstructure defects that may occur during the implementation of the process is given. An important point is that the authors emphasize the possibility of forming anisotropy of mechanical characteristics when using this technology. However, the paper did not consider the issue of the formation of characteristics of titanium alloys in particular.

The authors of paper [4] consider the influence of the scanning speed of the electron beam on the process of additive forming of an article from Ti-6Al-4V alloy powder. They come to the conclusion that an increase in the scanning speed in the studied range leads to an increase in the strength characteristics of the alloy. However, the authors do not provide other energy parameters of the process, so the transfer of these data to other systems requires additional research.

In work [5], authors investigate the same issue and come to similar conclusions but the lack of information about other parameters of the process does not make it possible to use these recommendations.

The authors of paper [6] consider the peculiarities of the processes of sintering and melting of metal powders under the influence of an electron beam during the implementation of the Electron Beam Powder Bed Fusion process. It is important that in the process of additive formation of the article at a relatively low beam energy, the flow of sintering processes (fusion) is possible. When the power of the beam is increased, the process of melting of the powder particles begins. The authors note that obtaining a non-porous material in the sintering process requires a significant exposure time, therefore, for a significant reduction in porosity, the melting mode is essential.

A systematic study of the influence of the parameters of the technological process of electron beam melting on the properties of the Ti-6Al-4V alloy is given in works [7, 8]. The authors consider the influence of such parameters as distance from build plate and part size [7] and energy input, orientation, and location [8]. The authors claim that there is a wide range of the specified parameters within which the set of mechanical characteristics remains stable. According to the authors, the geometric scheme of the sample formation has the greatest influence on the mechanical properties, which can lead to the formation of significant anisotropy of the mechanical characteristics. This coincides with the data in [3] but is in some contradiction with the data from [4], in which an increase in strength was noted with an increase in the scanning speed of the electron beam. At the same time, the authors of [9] believe that the presence or absence of defects (porosity, microcracks) exerts the main influence on the mechanical properties of titanium alloys obtained by the 3D printing method. Their appearance is an indicator of suboptimal technological parameters. In addition, the results reported in [7, 8] were obtained during the study of the Ti-6Al-4V alloy and cannot be directly transferred to other titanium alloys.

From our review of the literature, it follows that the use of electron beam melting technology for 3D printing of articles from titanium alloys is promising from the point of view of the possibility of obtaining products of complex shape with high mechanical characteristics [10]. But in order to implement the potential advantages of this technology, it is necessary to determine specific parameters of the process for this alloy and the features of the equipment used. In addition, most researchers indicate the danger of the formation of spatial anisotropy of mechanical characteristics,

which depends on the pattern of article formation. Therefore, further research should be directed to the optimization of the 3D printing process for the specified alloy, taking into account the specified features.

This will make it possible to obtain articles with a shape and dimensions close to the final ones, and with improved mechanical characteristics compared to the cast state.

## 3. The aim and objectives of the study

The purpose of our research is to find rational technological modes for 3D printing of blanks from the TA15 titanium alloy of the Ti-6.5Al-2Zr-1Mo-1V alloying system, which will make it possible to manufacture articles with a dense macrostructure and improved mechanical characteristics by the additive method.

To achieve the goal, the following tasks were set:

– to obtain test samples according to various printing technological parameters;

– to investigate the microstructure of articles;

– to devise printing modes that enable the formation of a dispersed homogeneous microstructure with no defects in the form of discontinuities;

– to determine mechanical characteristics of the experimental samples in comparison with the samples produced by the technology of electron beam remelting.

## 4. The study materials and methods

### 4. 1. The object and hypothesis of the study

The object of our research is the additive process of manufacturing articles from TA15 titanium alloy powder by the electron beam surfacing method. The hypothesis of the study assumed that since the Ti-6.5Al-2Zr-1Mo-1V system alloys have a very narrow liquidus-solidus temperature range, the mechanism of the material formation process from the powder would demonstrate a gradual transition from solid-phase sintering to melting. A change in the mechanism of the process will be accompanied by a corresponding change in the macrostructure of the metal. Therefore, the parameters of the process must be selected according to such indicators as the absence of macrodefects of the porosity type while preserving the maximally dispersed microstructure. It was assumed that the excessive specific energy received by the volume of the fused material leads to a coarsening of the dendritic structure of the formed material and, accordingly, to a decrease in the mechanical characteristics of the resulting workpiece. Therefore, parameters such as electron beam power, scanning speed, scan line displacement step, and powder layer thickness can be tools of influence on material formation processes. Variation in these parameters leads to a change in the specific energy values per unit volume of the fused powder and, accordingly, changes the kinetics of melting and subsequent crystallization. Therefore, in order to choose the rational parameters of the mode of 3D printing of the TA15 titanium alloy, it is necessary to carry out a comprehensive study on the influence of features in the formation of the macro- and microstructure on the set of mechanical characteristics of the alloy.

### 4. 2. Materials and equipment

The TA15 titanium alloy powder was used for the research, which was produced by the method of plasma melting and centrifugal spraying (PREP technology). Powder granules have a regular spherical shape with sizes from 45 to 113 microns. The chemical composition of the powder is given in Table 1.

Samples for research were made by layer-by-layer electron-beam 3D printing on experimental equipment (Fig. 1), designed at the Institute of Electric Welding named after E. O. Paton (Ukraine) [11].

The surfacing process took place in vacuum chamber 1 of the electron beam equipment (Fig. 1). The accelerating voltage of electron beam gun 2 was 60 kV. Preheating of the powder layer to a temperature of 730 °C was carried out by a raster beam with a power of 1800 W at a scanning speed of 14.6 m/s (an 8-pass rastering scheme was used). The working pressure in the vacuum chamber during surfacing was $10^{-4}$ Torr.

Table 1

Chemical composition of TA15 alloy powder, % (wt.)

| Al | V | Zr | Mo | Fe | Si | O | C | N | H | Ti |
|---|---|---|---|---|---|---|---|---|---|---|
| 5.5–7.1 | 0.8–2.5 | 1.5–2.5 | 0.5–2.0 | ≤0.25 | ≤0.15 | ≤0.15 | ≤0.08 | ≤0.05 | ≤0.015 | Balance |


Fig. 1. Experimental setup for electron beam 3D printing: 1 — vacuum chamber; 2 — electron beam gun; 3 — control cabinets; 4 — high-voltage source

To determine the metal structures, 25 samples (Fig. 2) were printed with a size of 25×25 mm, a height of 7.5 mm, where 2.5 mm are technological supports and 5 mm are the body of the article.

To study mechanical characteristics, 18 experimental samples (Fig. 3) with a width of 12 mm, a length of 62 mm, and a height of 14.5 mm were printed, of which 2.5 mm are technological supports.

The resulting blanks were used to make specimens for uniaxial tensile and impact bending tests. The mode of printing the samples for determining the mechanical properties was chosen based on the results of our study on the macro- and microstructure of the samples for metallographic studies. To compare the microstructure, samples of the TA15 alloy obtained by electron beam melting technology with an intermediate capacity and portioned supply of liquid metal to a water-cooled crystallizer were also selected. The implementation of this technology is described in [12].

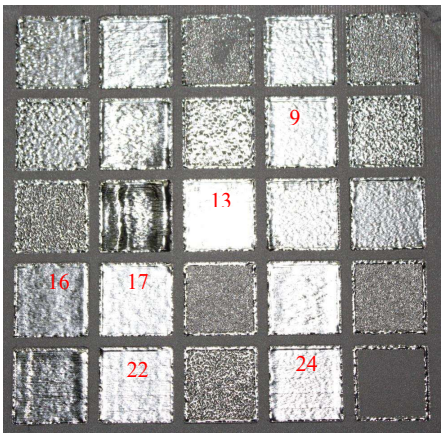


Fig. 2. Experimental samples for metallographic research

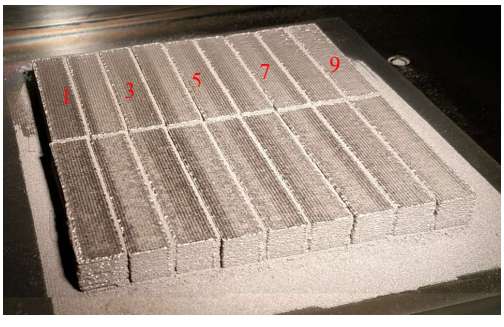


Fig. 3. Specimens for mechanical tests

**4. 3. Research methods**

The microstructure of the samples was studied using conventional methods. Transverse cuts were made on an EDM machine, which were sanded with sandpaper and polished with a diamond slurry. The surfaces were etched with an aqueous solution of 15 % $HNO_3$ and 5 % HF. The structures were examined using a Neophot-32 optical microscope (Germany). The image was recorded with an Olympus (Japan) camera.

To study the mechanical characteristics, blanks 12×12×60 mm in size were used, made by the electron-beam 3D printing method [13] and cut from a TA15 titanium alloy ingot obtained by electron-beam melting technology [12, 14].

Uniaxial tensile tests were performed on the MTS 318.25 universal servo-hydraulic test rig with a maximum force of 250 kN. Proportional samples with a diameter of 5 mm with a cylindrical working part were made from the blanks in accordance with the ISO 6892-1:2019 standard.

Tests were conducted in line with ISO 6892-1:2019. The load speed was controlled by the movement of the active gripper of the testing machine. For a more accurate determination of the conditional yield strength of the base metal, the speed of movement of the gripper on the linear section of the "stress-strain" diagram and in the zone of elastic-plastic deformation was 2 mm/min. At this stage, an extensometric sensor MTS 632.27F-20 with a deformation measurement base of 25 mm was used. The measurement accuracy was 0.001 mm, the measurement base was 25 mm. Subsequently, the speed of loading until the sample was destroyed was 10 mm/min.

Impact bending tests were performed by the Charpy method in accordance with ISO 148-1:2016 at room temperature on a KM-30 pendulum head with an automatic electric drive for lifting the pendulum. For the tests, blanks from the TA15 alloy were used, which were later milled and subjected to grinding. The height of the samples was 10 mm, the height of surface irregularities did not exceed 1.25 μm. Cuts on the samples with a width and depth of 2 mm were made on a milling machine.

## 5. Results of examining experimental samples

**5. 1. Obtaining experimental samples according to various printing technological parameters**

Samples for metal structure studies (Fig. 1) were printed from TA15 titanium alloy powder. The speed of the electron beam was 500 mm/s. The thickness of the metal powder layer was 100 μm. The scanning strategy is bidirectional, serpentine. The step of displacement of the beam trajectory changed from 0.1 to 0.25 mm with an interval of 0.05 mm. At the same time, the scanning direction was rotated by 90° for each layer. The energy density of the electron beam varied from 20 to 70 J/mm$^3$ for each value of the trajectory displacement step. A description of the technological parameters of surfacing and their relationship is given in [13, 15].

The condition of the surface of the samples was assessed visually. The initial inspection of the surfaces allowed us to divide the samples into four groups: unmelted, with a mosaic structure, fused with individual defects, fused without noticeable defects. The conformity of technological parameters of printing and the state of the surface of the samples are shown in Fig. 4.

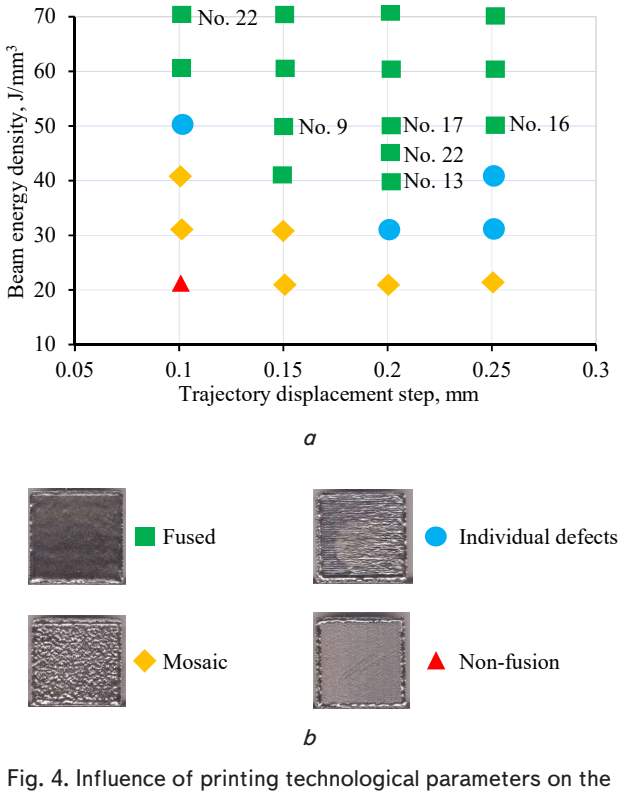


Fig. 4. Influence of printing technological parameters on the surface morphology of samples: *a* — grouping of samples according to the type of surface morphology; *b* — the morphology of the surface of samples, which underlies the grouping

Data in Fig. 4 demonstrate that the high surface quality (type of morphology – fused) was obtained when using different combinations of technological parameters. This

surface morphology was formed at certain values of energy density in the range of 40–70 J/mm$^3$ and a displacement in the trajectory of 0.1–0.25 mm. For further research, samples No. 9, 13, 16, 17, 22 with the highest surface quality were selected. Sample numbers in Fig. 4*a* correspond to the state of the surface shown in Fig. 2. Their 3D printing modes have low values of energy density and high values of trajectory displacement. These modes are promising from the point of view of reducing energy consumption and increasing printing speed.

**5. 2. Studying the microstructure of samples**

For our analysis of the metal structure, we selected samples obtained by 3D printing from TA15 titanium alloy powder without surface defects after surfacing (Fig. 4). In the studied samples, the following zones were distinguished to evaluate the features of the material structure:

– the substrate on which the samples were formed;

– base metal;

– surface.

In addition, the microstructure in the zone of the base metal was considered at increased magnification, as well as some features of the structure of individual samples. Fig. 5 shows the structures of the investigated samples in the substrate area.

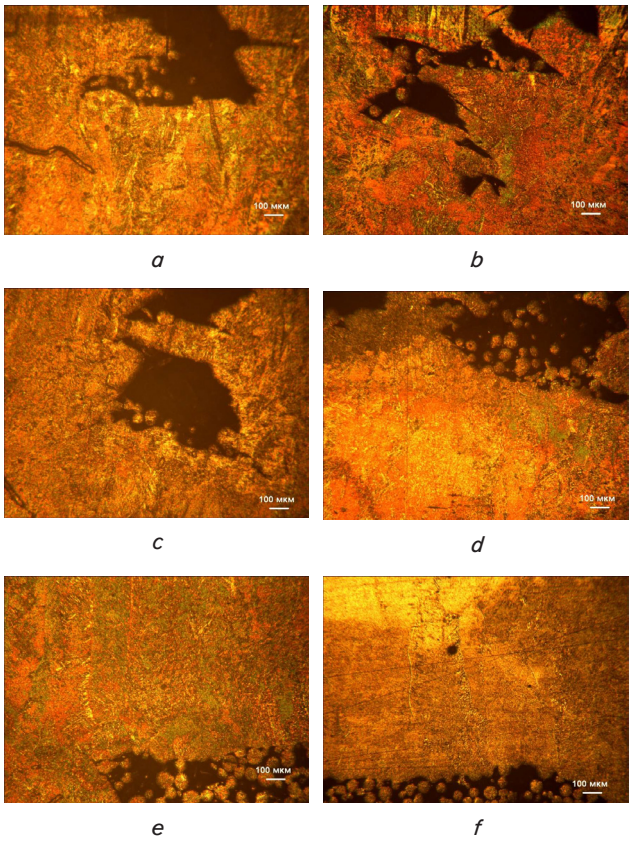


Fig. 5. Structure of samples in the area of the substrate (×100): *a* – sample No. 13; *b* – sample No. 16; *c* – sample No. 17; *d* – sample No. 22; *e* – sample No. 24; *f* – sample No. 9

In general, the microstructure is typical of the TA15 alloy and consists of α'-phase crystals with a needle-like morphology and a small amount of β-phase. All samples are characterized by the presence of discontinuities in the area of contact with the substrate, and individual particles of the powder used for printing can be observed in these discontinuities. The presence of discontinuities is associated with the peculiarities of the formation of technological supports with a thickness of 0.5 mm in the form of a lattice with a side of 3 mm. However, there are some differences in the general morphology of the structure of these zones

In samples No. 13 (Fig. 5, *a*), No. 16 (Fig. 5, *b*), No. 17 (Fig. 5, *c*), and No. 22 (Fig. 5, *d*), the formation of discontinuities of an irregular shape is visible, in which a small number of particles are observed. The discontinuities themselves have macro dimensions (1–2 mm) and their formation may be associated with non-melting of powder particles on the surface of the substrate. But in the areas where the melting took place, the formation of a continuous structure without signs of porosity is observed. The microstructure of the material is very dispersed, there is no apparent predominant grain orientation. This is due to the complete melting of the powder particles followed by very rapid crystallization, which leads to the formation of a dispersed non-directional structure. At the same time, sample No. 13 has the most inhomogeneous microstructure with the formation of relatively coarse separations of the α-phase, and further in the sequence of samples No. 16, 17, 22, this inhomogeneity decreases.

In samples No. 24 (Fig. 5, *e*) and No. 9 (Fig. 5, *f*), individual macro discontinuities in the substrate zone are not observed. The number of spherical particles associated with the molten metal increases; the zone of rapid crystallization adjacent to the substrate becomes less extensive. Signs of the formation of an oriented dendritic structure appear. The orientation of the longitudinal axes of the dendrites is perpendicular to the substrate, which coincides with the direction of heat removal. The structure of sample No. 9 is particularly characteristic in this case, where the formation of dendrites begins practically from the substrate, and the zone of dispersed unoriented structure is practically absent. Also, only in this sample is the formation of secondary shrinkage porosity in the interdendritic areas. Pores are single, spherical in shape, and 30–50 μm in diameter.

Changes in the morphology of the zone adjacent to the substrate are related to the difference in the specific energy introduced into the material during the printing process. An increase in energy leads to an improvement in the penetration of particles in the immediate vicinity of the substrate and greater homogeneity of the microstructure, but an excessive intensity of melting leads to the formation of coarse dendrites and secondary shrinkage porosity (sample No. 9).

Samples No. 22, 24 can be considered the best from the point of view of localization of macro discontinuities and homogeneity of the microstructure.

Fig. 6 shows a photograph of the dendritic structure that is formed in the base metal.

It can be seen that a change in the surfacing mode leads to changes in the parameters of the dendritic structure. The smallest transverse size of dendrites was recorded in sample No. 13 (Fig. 6, *a*), but sample No. 9 (Fig. 6, *b*) has similar parameters. But it should be noted that sample No. 9 is characterized by inhomogeneity, and the main metal has areas with a rough structure. Next, the size of the dendrites increases in sequence in samples No. 17 (Fig. 6, *d*), No. 22 (Fig. 6, *e*), No. 24 (Fig. 6, *f*). The maximum size of dendrites was formed in sample No. 16 (Fig. 6, *c*).

Fig. 7 shows the pattern of structure of the α'–β matrix of the alloy. It can be seen from the data in the Fig. 7

that all samples have a structure typical of pseudo α-alloys but differ in the dispersion of the mixture of acicular crystals. The most dispersed structure was formed in sample No. 13 (Fig. 7, *a*). Next, in order of decreasing dispersion, samples No. 16 (Fig. 7, *c*), No. 17 (Fig. 7, *d*), No. 22 (Fig. 7, *e*), No. 9 (Fig. 7, *f*), No. 24 (Fig. 7, *b*). It should be noted that the difference between samples No. 22, 9, 24 is small but they are significantly different from the group of samples No. 13, 15–17.

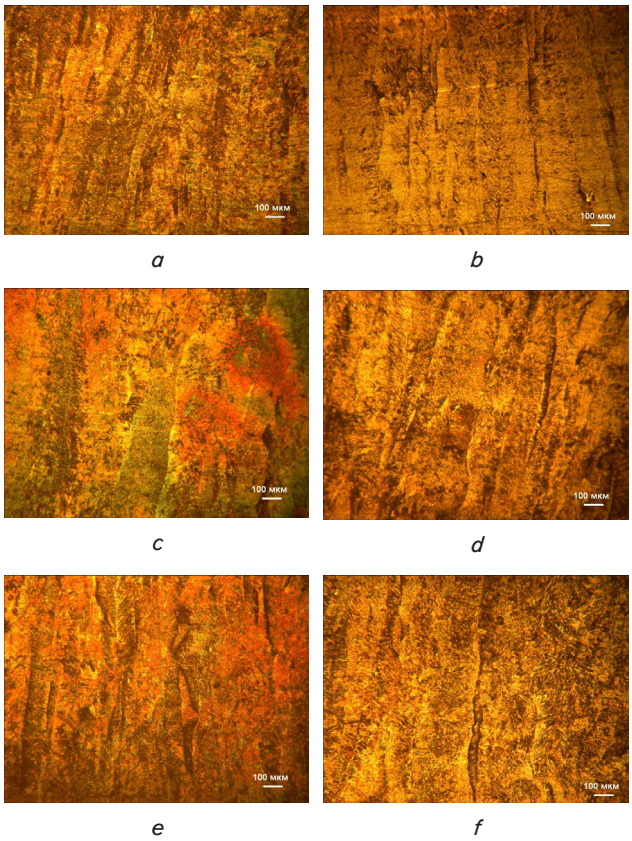


Fig. 6. Dendritic structure of the base metal of samples (×100): *a* – sample No. 13; *b* – sample No. 9; *c* – sample No. 16; *d* – sample No. 17; *e* – sample No. 22; *f* – sample No. 24

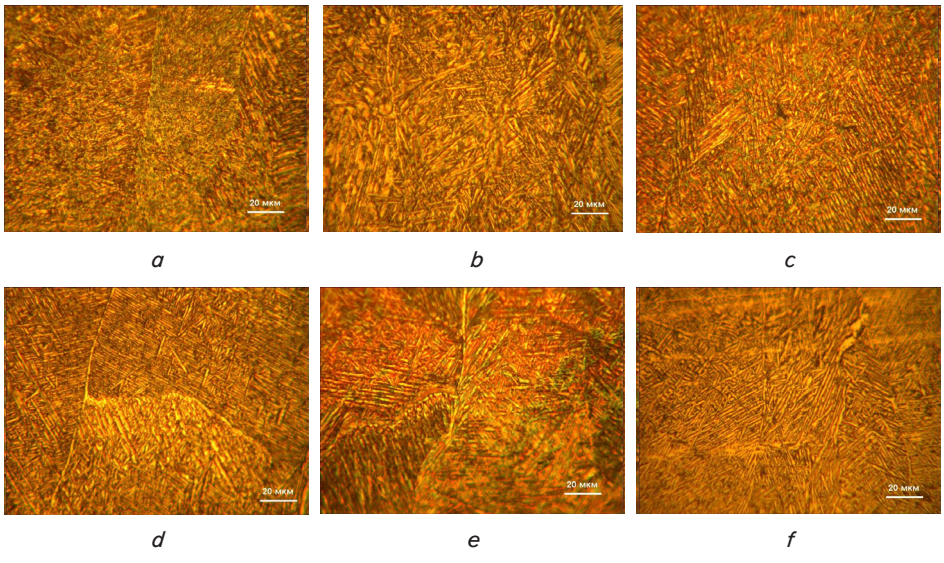


Fig. 7. Morphology of acicular crystals of the α' phase of the base metal (×500): *a* – sample No. 13; *b* – sample No. 24; *c* – sample No. 16; *d* – sample No. 17; *d* – sample No. 22; *f* – sample No. 9

Fig. 8 shows the comparative structures of materials obtained by electron beam 3D printing (Fig. 8, *a, b*) and electron beam melting (Fig. 8, *c, d*).

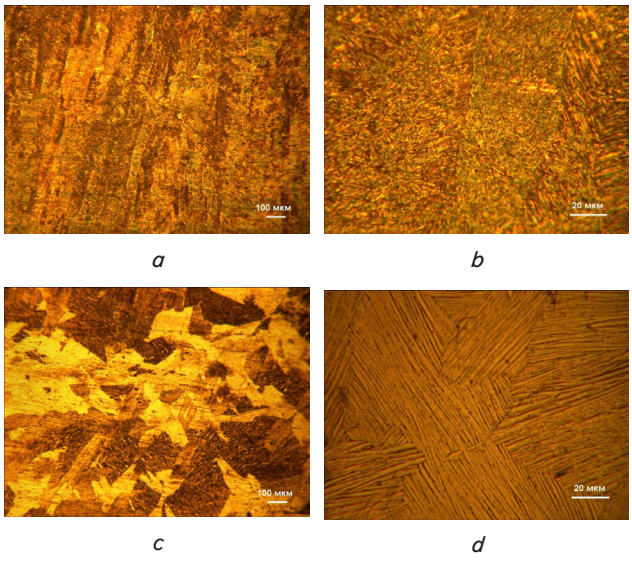


Fig. 8. Microstructure of TA15 alloy material: *a* – sample No. 13 (×100); *b* – sample No. 13 (×500) – electron beam 3D printing; *c* – (×100); *d* – (×500) – a sample obtained by electron beam melting

As can be seen from Fig. 8, the microstructure of the materials differs both at the level of the dendritic structure and at the level of the morphology of crystallites of α and β phases. The reasons for the formation of this difference and the influence of the features of the microstructure on the mechanical properties will be discussed further.

**5. 3. Establishing print modes that enable the formation of the best structural state**

When determining the printing modes that provide the best characteristics of the structure, it was established that sample No. 13 (Fig. 2) has the high quality surface (Fig. 2) with full penetration. It also has the most dispersed dendritic structure (Fig. 6) and the smallest size of α-phase acicular crystals (Fig. 7). It should be noted that for this sample, the formation of discontinuities of an irregular shape is observed in the area of the substrate (Fig. 6) but their length does not exceed 0.3–0.4 mm (Fig. 6).

From the data in Fig. 4, it follows that the mode of its 3D printing was carried out with a scanning step of 0.2 mm, the energy of the beam was 40 J/mm$^3$. This provides the lowest power consumption among samples with high surface quality and close to the maximum displacement of the scan path. Therefore, this mode was chosen for the production of specimens for mechanical tests.

**5. 4. Determining mechanical characteristics of experimental samples**

For research, samples were printed (Fig. 3), which were obtained by the 3D printing method from TA15 titanium alloy powder. The technological parameters of printing corresponded to the modes of sample No. 13 (Fig. 4). For comparisons of mechanical characteristics, samples made from a casting of TA15 titanium alloy obtained by electron beam melting technology were used.

The tests were carried out for uniaxial tension and impact bending.

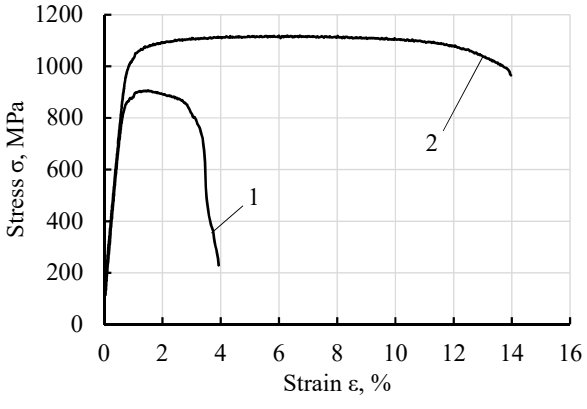


Fig. 9. Diagrams of deformation by uniaxial tension of samples of titanium alloys produced by the following methods: 1 — electron beam melting; 2 — electron beam 3D printing

**5. 4. 1. Uniaxial tension test**

Samples No. 1, 5, 9 (Fig. 2) obtained by the method of electron beam 3D printing and samples manufactured by the technology of electron beam melting were studied.

The mechanical characteristics of titanium alloys were determined by deformation diagrams (Fig. 9) in accordance with ISO 6892 1:2019. The average values of the characteristics of the mechanical properties of titanium alloys according to the results from uniaxial tensile testing of samples are given in Table 2.

From Table 2, it can be seen that the values of strength characteristics of the TA15 titanium alloy obtained by the EBP technology are 20 % higher than those of the cast metal of the TA15 alloy obtained by the EBM technology. Plasticity indicators when using EBP technology are 3.2 times higher compared to EBM technology.

Table 2

Mechanical characteristics of TA15 samples made by electron beam 3D printing (EBP) and electron beam melting (EBM) technologies

| Sample manufacturing technology | Tensile strength $R_m$, MPa | Yield strength $R_{0.2}$, MPa | Young's module $E$, GPa | Relative elongation $A_5$, % |
|---|---|---|---|---|
| EBP | 1139 | 1050 | 122 | 16,5 |
| EBM | 895 | 849 | 134 | 5,1 |

**5. 4. 2. Impact bending test**

We studied samples No. 3, 7 (Fig. 3), which were obtained by the electron beam 3D printing method, and samples made by the electron beam melting technology.

The tests were carried out by the Charpy method in accordance with ISO 148–1:2016. According to the results of the tests, the work spent on the destruction of the sample was determined, and the impact toughness was calculated. The results of impact bending tests are shown in Fig. 10.

From the diagram in Fig. 10, it can be seen that the value of impact toughness is KCU=55 J/cm$^2$ for samples made from

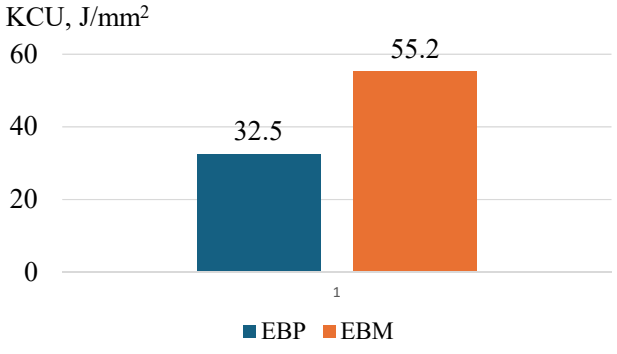


Fig. 10. Average values of impact toughness of samples made by electron beam 3D printing (EBP) and electron beam melting (EBM) technologies

a titanium alloy ingot using the electron beam melting (EBM) technology. This is almost twice as high as KCU=35 J/cm$^2$ for samples created by electron beam 3D printing (EBP). The reasons will be discussed in Chapter 6.

## 6. Discussion of results of investigating the structure and properties of TA15 alloy blanks obtained by 3D printing

From the results of visual inspection of the surface condition of the samples, it can be seen that in the studied range of changes in beam energy density and scanning trajectory displacement, the surface morphology changes in a wide range. Fig. 2 shows that it is possible to distinguish 4 types of surface condition (non-fusion, mosaic structure, presence of individual defects, fusion). The intervals for changing the technological parameters studied in the work made it possible to establish the interval for changing the energy density of the beam and the displacement value of the scanning trajectory, within which it is possible to obtain a material with a defect-free surface (Fig. 2). Within the specified interval, combinations of parameters were determined that ensure obtaining the high quality surface (Fig. 4).

Studies of the macro- and microstructure of the surfaced material showed that even in samples with a defect-free surface, the formation of defects of the non-melting type is observed in the zone that is in direct contact with the substrate (Fig. 5). This is due to the intensive removal of heat to the substrate at the first stages of sample formation. An increase in the specific energy of the beam (per unit of powder volume) helps reduce the manifestation of this defect but has negative consequences in the formation of a directed dendritic structure, which becomes coarser with an increase in the specific energy of the beam. At maximum energy values, secondary porosity may occur due to overheating of the melt and increased shrinkage during crystallization (Fig. 6). Therefore, in this case, it is necessary to find a rational ratio of process parameters. From the point of view of obtaining a dispersed structure of the main volume of the material and, as a result, increased mechanical characteristics, the process parameters should enable complete melting of the powder particles but not lead to the formation of the above defects (Fig. 7).

The choice of the 3D printing mode, which provides the best parameters of the macro- and microstructure, was also made taking into account the energy consumption of the process and its productivity. To increase energy efficiency, modes with the minimum value of the beam energy density should be selected, and the productivity of the process increases with increasing values of the displacement of the scanning trajectory. From the obtained data (Fig. 4–7) it follows that the printing mode of sample No. 13 is the most promising.

The rationality of this approach is confirmed by the results of mechanical tests. When choosing the mode of obtaining samples, the mode of obtaining sample 13 was taken as a basis. This mode made it possible to obtain the most dispersed microstructure among samples with complete penetration. At the same time, the formation of α-phase layers at the borders of dendrites is not observed in the structure of the sample. As a result of the formation of such a structure, it was possible to obtain mechanical properties during tensile tests with a strength limit value 27 % higher than that of an alloy melted by conventional electron beam melting technology. For the yield strength, the excess is 24 %, and the relative elongation of the material printed by 3D printing technology is 3.2 times higher (Fig. 9 and data in Table 2). This is explained by the formation of a dispersed structure due to slight overheating of the melt and rapid removal of excess heat into the previously crystallized layers of the material. This explanation is illustrated in Fig. 8.

From the comparison of the structures in Fig. 8, it can be seen that the 3D printing technology makes it possible to obtain a much more dispersed structure of crystallites of α and β phases. However, the sample obtained by 3D printing (Fig. 8, *a, b*) is characterized by the presence of a pronounced texture formed by equally oriented dendrites. The sample obtained by electron beam melting (Fig. 8, *c, d*) has an isotropic structure formed by relatively equiaxed grains. During static stretching, the dispersed structure provides an increase in strength and plasticity characteristics at the same time.

Our result is explained by the fact that, based on the main hypothesis of the research, the key parameter of the process is the specific energy of the beam. Its growth determines the transition from the mechanisms of sintering (fusion) to the melting of powder particles (melting). But after such a transition, the process of overheating of the melt and coarsening of the structure begins. Therefore, in contrast to the approach proposed in [4–6], the geometrical parameters of printing (scanning speed and trajectory displacement) are not the main ones but should be chosen under the condition of achieving optimal specific energy values. Moreover, these values have bilateral restrictions. Conducting the process under the melting mode should not lead to the start of processes of coarsening the structure. That is why, in contrast to recommendations [8], signs of an optimal structure are not only the absence of macrodefects but also a dispersed microstructure with the minimum possible distance between the axes of dendrites.

This is confirmed by the results of impact bending tests. In the case of unfavorable orientation of unidirectional dendrites relative to the direction of application of force during impact bending tests, a decrease in the values of this characteristic is possible. This effect was observed in this study (Fig. 10). This assumption is confirmed by the results obtained by the authors of [3, 7, 8]. Therefore, when designing articles obtained by the 3D printing method, it is necessary to take into account the direction of application of maximum shock loads and shape the article in such a way as to ensure the best orientation of the texture relative to the direction of the load.

It should be noted that with this 3D printing sample manufacturing scheme, the uniaxial tensile test was conducted in the most unfavorable direction of load application – across the orientation of the dendrites. Therefore, the value of the increase in mechanical characteristics can be even higher with a favorable direction of load application along the axes of the dendrites.

The influence of anisotropy on the value of impact toughness was revealed during the study, when the blanks for determining the properties during impact bending tests were already formed. Their dimensions did not allow us to produce samples with an orientation of dendrites relative to the direction of application of the load, which is different from the one studied in the work. Therefore, it was not possible to verify the above statement in the course of the current study. For this, in the future, it is necessary to produce samples in which the direction of growth of dendrites will be perpendicular to the direction of application of the load.

Our results can be used for further improvement of 3D printing modes of TA15 alloy articles. The proposed approach involves optimizing process parameters in order to obtain a dispersed structure with a rational orientation of dendrites relative to the direction of load application. It can be used to improve production modes of other alloys. The expected effect is to reduce the material consumption of the article production process with a simultaneous increase in the set of mechanical characteristics due to the use of optimized 3D printing technology.

The parameters that influence the formation of the dendritic structure also include the granulometric composition of the powder. In the study, it was kept unchanged, which somewhat limits the application of our results to cases of using powders of other granulometry. Research in this area should continue. Optimizing the granulometric composition of powders specifically for electron-beam 3D printing technology will make it possible to reduce the degree of development of unidirectional dendritic texture in the finished article. This, in turn, will make it possible to obtain a smaller anisotropy of the impact toughness values.

The disadvantage of this study worth noting is that when studying the relationship between structure and mechanical properties, fractographic analysis was not performed. A decrease in impact viscosity toughness may have other explanations besides the unfavorable orientation of dendrites. In the future, the use of scanning electron microscopy methods will make it possible to clarify the mechanism of destruction during impact bending and to devise effective methods for improving this characteristic.

## 7. Conclusions

1. Using electron beam 3D printing technology, 25 samples were obtained for structural studies and 18 samples for determining mechanical characteristics. The step of displacement of the beam trajectory changed from 0.1 to 0.25 mm with an interval of 0.05 mm. The specific energy of the electron beam varied from 20 to 70 J/mm$^3$ for each step value of trajectory displacement.

2. The obtained samples have a dendritic type of microstructure with α′+β lamellar-acicular morphology. Its

dispersity and the form of α′-phase discharge vary depending on the amount of specific energy introduced into the material during the printing process. At its low values, the formation of discontinuities of an irregular shape is observed in the zone adjacent to the substrate. Increasing energy leads to improved melting of particles in the immediate vicinity of the substrate and greater homogeneity of the microstructure but excessive melting intensity leads to the formation of coarse dendrites and secondary shrinkage porosity.

3. From the point of view of the formation of a favorable microstructure, the printing mode with a scanning step of 0.2 mm and a beam energy of 40 J/mm$^3$ makes it possible to obtain a dispersed microstructure of the material in which there are no non-melting and shrinkage micropores. This makes it possible to obtain an increased set of mechanical characteristics of the TA15 alloy.

4. The indicated mode ensures that the strength limit is obtained, higher by 27 %, and the yield point, 24 % higher, than those in the alloy made by the conventional technology of electron beam melting. The relative elongation of material printed by 3D printing technology is 3.2 times higher. This is due to the formation of a more dispersed microstructure. However, as a result of the formation of a unidirectional dendritic structure, there is a decrease in the impact bending test results with an unfavorable orientation of the sample in relation to the direction of load application.

## Conflicts of interest

The authors declare that they have no conflicts of interest in relation to the current study, including financial, personal, authorship, or any other, that could affect the study and the results reported in this paper.

## Funding

The work was funded within the framework of the target program of scientific research at the Ukraine's National Academy of Sciences on the topic "Development of technologies for obtaining novel titanium alloys by electron beam melting and articles from them by rolling and 3D printing for the needs of defense and medicine" (State registration number 0123U100870).

## Data availability

The data will be provided upon reasonable request.

## Use of artificial intelligence

The authors confirm that they did not use artificial intelligence technologies when creating the current work.

## Acknowledgments

The authors are grateful to the State Enterprise "Engineering Center for Electron Beam Welding" at the Institute of Electric Welding named after E.O. Paton of the National Academy of Sciences of Ukraine" for technical support in conducting research.

References

1. Murr, L. E., Gaytan, S. M., Ramirez, D. A., Martinez, E., Hernandez, J., Amato, K. N. et al. (2012). Metal Fabrication by Additive Manufacturing Using Laser and Electron Beam Melting Technologies. Journal of Materials Science & Technology, 28 (1), 1–14. https://doi.org/10.1016/s1005-0302(12)60016-4
2. Lai, X., Yang, G., Wang, Y., Wei, Z. (2023). Heat and mass transfer in electron beam additive manufacturing. International Journal of Mechanical Sciences, 259, 108613. https://doi.org/10.1016/j.ijmecsci.2023.108613
3. Shi, Y., Gong, S., Xu, H., Yang, G., Qiao, J., Wang, Z. et al. (2023). Electron beam metal additive manufacturing: Defects formation and in-process control. Journal of Manufacturing Processes, 101, 386–431. https://doi.org/10.1016/j.jmapro.2023.06.013
4. Wang, X., Gong, X., Chou, K. (2015). Scanning Speed Effect on Mechanical Properties of Ti-6Al-4V Alloy Processed by Electron Beam Additive Manufacturing. Procedia Manufacturing, 1, 287–295. https://doi.org/10.1016/j.promfg.2015.09.026
5. Wang, X., Chou, K. (2018). EBSD study of beam speed effects on Ti-6Al-4V alloy by powder bed electron beam additive manufacturing. Journal of Alloys and Compounds, 748, 236–244. https://doi.org/10.1016/j.jallcom.2018.03.173
6. Batalha, G. F., Silva, L. C., Coelho, R. S., Teixeira, M. C. C., Castro, T. L., Pereira, M. V. S. et al. (2024). Mechanical properties characterization of Ti-6Al-4 V grade 5 (recycled) additively manufactured by selective electron beam melting (EB-PBF). Engineering Failure Analysis, 157, 107892. https://doi.org/10.1016/j.engfailanal.2023.107892
7. Hrabe, N., Quinn, T. (2013). Effects of processing on microstructure and mechanical properties of a titanium alloy (Ti–6Al–4V) fabricated using electron beam melting (EBM), part 1: Distance from build plate and part size. Materials Science and Engineering: A, 573, 264–270. https://doi.org/10.1016/j.msea.2013.02.064
8. Hrabe, N., Quinn, T. (2013). Effects of processing on microstructure and mechanical properties of a titanium alloy (Ti–6Al–4V) fabricated using electron beam melting (EBM), Part 2: Energy input, orientation, and location. Materials Science and Engineering: A, 573, 271–277. https://doi.org/10.1016/j.msea.2013.02.065
9. Tamayo, J. A., Riascos, M., Vargas, C. A., Baena, L. M. (2021). Additive manufacturing of Ti6Al4V alloy via electron beam melting for the development of implants for the biomedical industry. Heliyon, 7 (5), e06892. https://doi.org/10.1016/j.heliyon.2021.e06892

10. Matviichuk, V. A., Nesterenkov, V. M., Berdnikova, O. M. (2022). Additive electron beam technology of manufacture of metal products from powder materials. Avtomaticheskaya Svarka (Automatic Welding), 2022 (2), 16–25. https://doi.org/10.37434/as2022.02.03
11. Matviichuk, V. A., Nesterenkov, V. M. (2020). Additive electron beam equipment for layer-by-layer manufacture of metal products from powder materials. The Paton Welding Journal, 2020 (2), 41–46. https://doi.org/10.37434/tpwj2020.02.08
12. Akhonin, S., Pikulin, O., Berezos, V., Severyn, A., Erokhin, O., Kryzhanovskyi, V. (2022). Determining the structure and properties of heat-resistant titanium alloys VT3-1 and VT9 obtained by electron-beam melting. Eastern-European Journal of Enterprise Technologies, 5 (12 (119)), 6–12. https://doi.org/10.15587/1729-4061.2022.265014
13. Matviichuk, V., Nesterenkov, V., Berdnikova, O. (2022). Determining the influence of technological parameters of the electron-beam surfacing process on quality indicators. Eastern-European Journal of Enterprise Technologies, 1 (12 (115)), 21–30. https://doi.org/10.15587/1729-4061.2022.253473
14. Akhonin, S. V., Pikulin, O. M. (2019). Investigation of Effect of Electron Beam Surface Treatment of Titanium Alloy Ingots on Structure and Properties of Melted Metal. IOP Conference Series: Materials Science and Engineering, 582 (1), 012047. https://doi.org/10.1088/1757-899x/582/1/012047
15. Matviichuk, V., Nesterenkov, V., Berdnikova, O. (2024). Determining the influence of technological parameters of electron beam surfacing process on the microstructure and microhardness of Ti-6Al-4V alloy. Eastern-European Journal of Enterprise Technologies, 1 (12 (127)), 6–12. https://doi.org/10.15587/1729-4061.2024.297773